Hindawi Publishing Corporation
EURASIP Journal on Wireless Communications and Networking
Volume 2009, Article ID 481214, 9 pages
doi:10.1155/2009/481214

Research Article

On Channel Estimation for OFDM/TDM Using MMSE-FDE in a Fast Fading Channel

Haris Gacanin and Fumiyuki Adachi

Department of Electrical and Communication Engineering, Graduate School of Engineering, Tohoku University, Sendai 980-8579, Japan

Correspondence should be addressed to Haris Gacanin, harisg@mobile.ecei.tohoku.ac.jp

Received 30 January 2009; Accepted 25 June 2009

Recommended by Yan Zhang

MMSE-FDE can improve the transmission performance of OFDM combined with time division multiplexing (OFDM/TDM), but knowledge of the channel state information and the noise variance is required to compute the MMSE weight. In this paper, a performance evaluation of OFDM/TDM using MMSE-FDE with pilot-assisted channel estimation over a fast fading channel is presented. To improve the tracking ability against fast fading a robust pilot-assisted channel estimation is presented that uses time-domain filtering on a slot-by-slot basis and frequency-domain interpolation. We derive the mean square error (MSE) of the channel estimator and then discuss a tradeoff between improving the tracking ability against fading and the noise reduction. The achievable bit error rate (BER) performance is evaluated by computer simulation and compared with conventional OFDM. It is shown that the OFDM/TDM using MMSE-FDE achieves a lower BER and a better tracking ability against fast fading in comparison with conventional OFDM.

1. Introduction

Orthogonal frequency division multiplexing (OFDM) is receiving considerable interest because of its high capacity and robustness against the channel frequency-selectivity [1]. OFDM signals, however, have a problem with a high peak-to-average power ratio (PAPR). OFDM combined with time division multiplexing (OFDM/TDM) [2] can reduce the PAPR, and furthermore, with the application of minimum mean square error frequency domain equalization (MMSE-FDE) it can bridge the performance of conventional OFDM and single carrier (SC)-FDE [3]. In OFDM/TDM, the inverse fast Fourier transform (IFFT) time window (i.e., OFDM/TDM frame) of conventional OFDM is divided into K slots; within each slot an OFDM signal with reduced number of subcarriers is transmitted. At the receiver, MMSE-FDE is applied over the entire frame to exploit the channel frequency-selectivity. MMSE-FDE, however, requires knowledge of the channel state information and the noise variance.

Various channel estimation techniques for conventional OFDM and SC-FDE have been presented in [4–11]. There are two approaches to estimate the channel state information. In one approach, the channel estimation is done by time-domain multiplexed pilot (TDM-pilot), but the tracking ability against fast fading degrades. In another approach, the channel estimation is done by frequency-domain multiplexed pilot (FDM-pilot) to improve the tracking ability against fast fading, but the bit error rate (BER) increases due to increased noise after frequency-domain interpolation. To date, the effect of channel estimation on the performance of OFDM/TDM using MMSE-FDE has not been fully discussed.

This paper deals with the channel estimation for OFDM/TDM using MMSE-FDE over a fast fading channel. We adopt a pilot-structure for SC transmission [8] and apply recursive least-square (RLS) algorithm [12] in time domain (in this paper called time-domain first-order filtering (TDFF)) on a slot-by-slot basis within the OFDM/TDM frame to improve the tracking ability against fast fading. We develop an expression for the mean square error (MSE) of the channel estimator and then discuss a tradeoff between improvement of the tracking ability against fast fading and

the noise reduction. The BER performance improvement is achieved through the frequency diversity gain and improved tracking ability against fast fading without sacrificing transmission data-rate.

The rest of the paper is organized as follows. In Section 2, we describe the system model. Pilot-assisted channel estimation techniques are presented in Section 3, while the estimator performance analysis is presented in Section 4. We evaluate the performance by computer simulation in Section 5. Section 6 concludes the paper.

2. System Model

The OFDM/TDM system model is illustrated in Figure 1. Throughout this paper, T_c-spaced discrete-time signal representation is used, where T_c represents FFT sampling period.

The gth signaling interval of the conventional OFDM with N_c subcarriers is divided into K slots (i.e., gth OFDM/TDM frame) as shown in Figure 2. A sequence of N_c data-modulated symbols in the gth frame $\{d_g(i);\ i = 0 \sim N_c - 1\}$ is divided into K blocks of $N_m\ (= N_c/K)$ data-modulated symbols each. The kth block symbol sequence in the gth frame is denoted by $\{d_g^k(i);\ i = 0 \sim N_m - 1\}$, where $d_g^k(i) = d_g(kN_m + i)$ for $k = 0 \sim K - 1$ with $E[|d_g(i)|^2]$=1 ($E[\cdot]$ is the ensemble average operation). The gth frame OFDM/TDM signal can be expressed using the equivalent lowpass representation as

$$s_g(t) = \sqrt{\frac{2E_s}{T_c N_m}} \sum_{i=0}^{N_m-1} d_g^{\lfloor t/N_m \rfloor}(i) \exp\left\{ j2\pi t \frac{i}{N_m} \right\} \qquad (1)$$

for $t = 0 \sim N_c - 1$, where $\lfloor x \rfloor$ and E_s, respectively, denote the largest integer smaller than or equal to x and the data-modulated symbol energy. We note here that OFDM/TDM signal with $K = 1$ (i.e., $N_m = N_c$) reduces to the conventional OFDM system with N_c subcarriers. After insertion of an N_m-sample guard interval (GI), the OFDM/TDM signal is transmitted over a fading channel.

The gth frame OFDM/TDM signal propagates through the channel having a discrete-time channel impulse response $h_g(\tau)$ given as

$$h_g(\tau) = \sum_{l=0}^{L-1} h_{g,l}\delta(\tau - \tau_l), \qquad (2)$$

where $h_{g,l}$ and τ_l, respectively, denotes the gth frame's path gain and the time delay of the lth path having the sample-spaced exponential power delay profile with channel decay factor α (i.e., $E[|h_{g,l}|^2] = ((1-\alpha)/(1-\alpha^L))\alpha^l$). The maximum time delay of the channel is assumed to be less than the GI length.

The received gth frame OFDM/TDM signal is represented by $\{r_g(t);\ t = -N_m \sim N_c - 1\}$. After removal of the GI, $\{r_g(t);\ t = 0 \sim N_c - 1\}$ is fed to N_c-point FFT to decompose the received signal into N_c frequency components $\{R_g(n);\ n = 0 \sim N_c - 1\}$ given by

$$R_g(n) = S_g(n)H_g(n) + I_g(n) + N_g(n), \qquad (3)$$

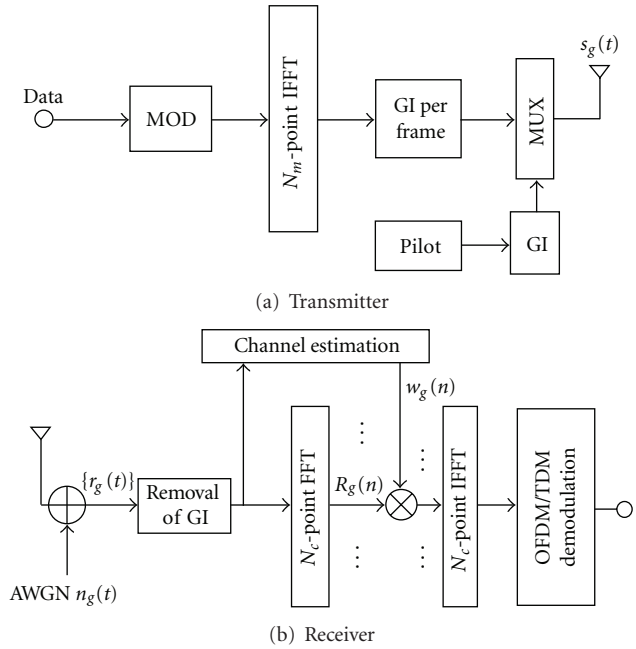

Figure 1: OFDM/TDM transmitter/receiver structure.

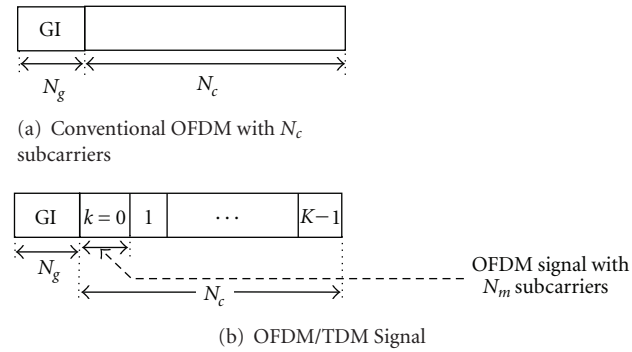

Figure 2: OFDM/TDM frame structure.

where $S_g(n)$, $H_g(n)$, $I_g(n)$, and $N_g(n)$, respectively, denote the Fourier transforms of the gth frame transmit OFDM/TDM signal, the channel impulse response, the inter-slot interference (ISI) and the additive white Gaussian noise (AWGN) having single sided power spectral density N_0. Note that in case of conventional OFDM ($K = 1$) the ISI term vanishes.

One-tap MMSE-FDE similar to SC-FDE [8] is applied over the entire frame with K concatenated OFDM signals as [3]

$$\begin{aligned} \hat{R}_g(n) &= R_g(n)W_g(n) \\ &= S_g(n)\hat{H}_g(n) + \hat{I}_g(n) + \hat{N}_g(n) \end{aligned} \qquad (4)$$

with $\hat{H}_g(n) = H_g(n)W_g(n)$ and $\hat{I}_g(n) = I_g(n)W_g(n)$, where $W_g(n)$ denotes the MMSE equalization weight given by

$$W_g(n) = \frac{H_g^*(n)}{\left|H_g(n)\right|^2 + 2\sigma_g^2}, \qquad (5)$$

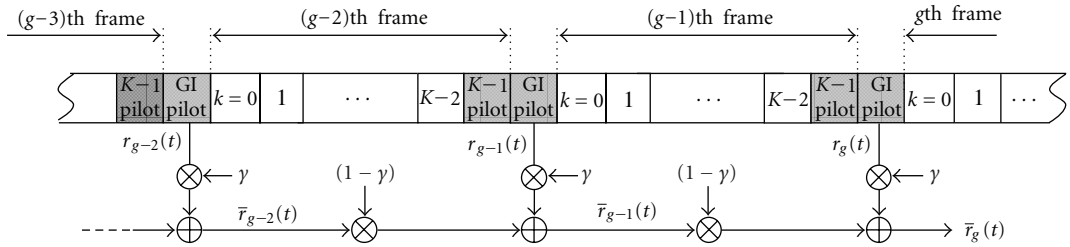

Figure 3: Time-domain first-order filtering.

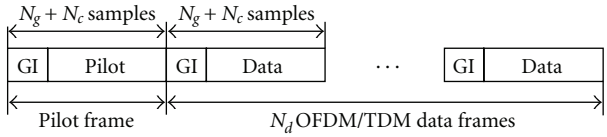

Figure 4: OFDM/TDM pilot block insertion.

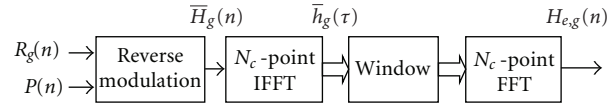

Figure 5: Pilot-assisted channel estimation using time-delay domain windowing.

where σ_g^2 and $(\cdot)^*$ denote the noise variance and the complex conjugate operation, respectively. We need to estimate $H_g(n)$ and σ_g^2. Channel estimation techniques will be described in the following section.

The time-domain OFDM/TDM signal is recovered by applying N_c-point IFFT to $\{\hat{R}(n);\ n = 0 \sim N_c - 1\}$, and then, the demodulation of OFDM signals with N_m subcarriers is done by N_m-point FFT [3].

3. Channel Estimation

The channel and the noise variance in OFDM/TDM system can be estimated with TDM-pilot, but the tracking ability significantly degrades in a fast fading channel [13]. To improve tracking against fast fading the channel estimation with FDM-pilot [5] can be directly applied to OFDM/TDM, but the GI must be inserted between the slots within the OFDM/TDM frame that will reduce the data-rate and the frequency diversity gain cannot be obtained. Former is due to the fact that the GI length must be kept the same as conventional OFDM, while latter is because the insertion of GI will destroy the property of OFDM/TDM. Moreover, if FDM-pilot is directly applied to OFDM/TDM, the received pilot subcarriers within the slots will be corrupted by ISI (see (4)) leading to the estimator performance degradation.

We focus on three estimation schemes: (i) channel estimation with TDM-pilot and time-domain first-order filtering (TDFF), (ii) channel estimation with TDM-pilot [13], and (iii) channel estimation with FDM-pilot [5]. These methods are described next (note that our aim is to keep the transmission data-rate the same as conventional OFDM). Then, pilot signal selection and noise variance estimation are discussed.

3.1. Channel Estimation with TDM-Pilot and TDFF. The pilot signal $\{p(i);\ i = 0 \sim N_m - 1\}$ is inserted into $(K-1)$th slot (i.e., $d^{K-1}(i) = p(i)$ for $i = 0 \sim N_m - 1$) and into the GI as a cyclic prefix as illustrated in Figure 3. Since the same pilot is used for all frames, the $(g-1)$th frame's pilot slot acts as a cyclic prefix for the gth frame's GI. Thus, the channel estimation can be performed using the gth frame's N_m-sample GI. Similar frame structure was presented for SC transmission in [8]. The channel gain estimate and noise variance estimate to be used for FDE are denoted by $H_{e,g}(n)$ and $2\sigma_{e,g}^2$, respectively. $H_g(n)$ and σ_g^2 in (5) are replaced by $H_{e,g}(n)$ and $\sigma_{e,g}^2$, respectively.

The received pilot $\{r_g(t);\ t = -N_m \sim -1\}$ in the GI is filtered on a slot-by-slot basis by the time-domain first-order filtering as illustrated in Figure 3 to increase the signal-to-noise power ratio (SNR) of the pilot signal. The filtered pilot signal is obtained as

$$\bar{r}_g(t) = \gamma r_g(t) + (1-\gamma)\bar{r}_{g-1}(t) \tag{6}$$

for $t = -N_m \sim -1$, where γ is the forgetting factor with the initial condition $\bar{r}_0(t) = r_0(t)$. Then, N_m-point FFT is applied to decompose $\{\bar{r}_g(t);\ t = -N_m \sim -1\}$ into N_m subcarrier components $\{\overline{R}_g(q);\ q = -N_m \sim -1\}$ as

$$\overline{R}_g(q) = \sum_{t=-N_m}^{-1} \bar{r}_g(t) \exp\left\{-j2\pi q \frac{t}{N_m}\right\} \tag{7}$$

with $q = \lfloor n/K \rfloor$ for $n = 0 \sim N_c - 1$ and the initial condition $\overline{R}_0(q) = R_0(q)$. The instantaneous channel gain estimate at the qth subcarrier is obtained by removing the pilot modulation as

$$\overline{H}_g(q) = \frac{\overline{R}_g(q)}{P(q)} = H_g(q) + \tilde{N}_g(q), \tag{8}$$

where $\tilde{N}_g(q) = N_g(q)/P(q)$ and $P(q)$ denotes the qth frequency component of $\{p(t);\ t = 0 \sim N_m - 1\}$.

Since $q = \lfloor n/K \rfloor$, the channel estimates are obtained only at the frequencies $n = 0, N_m, 2N_m, \ldots, (N_c - 1)$ as shown in Figure 6. Hence, an interpolation is necessary to obtain the channel gains for all frequencies (i.e., $n = 0 \sim N_c - 1$). We

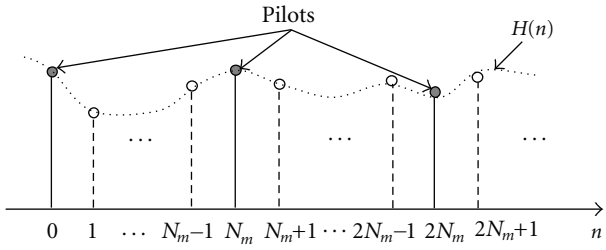

Figure 6: Pilot frequencies.

apply the following frequency-domain interpolation. First, N_m-point IFFT is performed on $\{\overline{H}_g(q);\ q = 0 \sim N_m - 1\}$ to obtain the instantaneous channel impulse response $\{\overline{h}(\tau);\ \tau = 0 \sim N_m - 1\}$ as

$$\overline{h}_g(\tau) = \frac{1}{N_m} \sum_{q=0}^{N_m-1} \overline{H}_g(q) \exp\left\{ j2\pi\tau \frac{q}{N_m} \right\}. \tag{9}$$

Then, N_c-point FFT is applied to obtain the interpolated channel gain estimates $\{H_{e,g}(n);\ n = 0 \sim N_c - 1\}$ for all N_c frequencies as

$$H_{e,g}(n) = \sum_{\tau=0}^{N_m-1} \overline{h}_g(\tau) \exp\left\{ -j2\pi n \frac{\tau}{N_c} \right\}. \tag{10}$$

3.2. Channel Estimation with TDM-Pilot. For OFDM/TDM with pilot-assisted channel estimation using TDM-pilot [13], a pilot signal is transmitted followed by N_d OFDM/TDM data frames is illustrated in Figure 4. The block diagram of channel estimation is illustrated in Figure 5. Notice that in this case all N_c subcarriers are used as pilots.

First, by reverse modulation, the instantaneous channel gain estimate $\overline{H}_g(n)$ at the nth subcarrier is obtained by (8). Then, N_c-point IFFT is applied to $\{\overline{H}_g(n);\ n = 0 \sim N_c - 1\}$ to obtain the instantaneous channel impulse response $\{\overline{h}(\tau);\ \tau = 0 \sim N_c - 1\}$. Assuming that the actual channel impulse response is present only within the GI, the estimated channel impulse response beyond the GI is replaced with zeros to reduce the noise [11]. Finally, N_c-point FFT is applied to obtain the improved channel gain estimates $\{H_{e,g}(n);\ n = 0 \sim N_c - 1\}$.

3.3. Channel Estimation with FDM-Pilot. For pilot-aided channel estimation with FDM-pilot [5] using frequency-domain interpolation an N_m equally-spaced pilot subcarriers among N_c subcarriers are used.

First, by reverse modulation, the instantaneous channel gain estimate $\{\overline{H}_g(q);\ q = \lfloor n/N_m \rfloor$ for $n = 0 \sim N_c - 1\}$ at the pilot subcarriers is obtained by (8), where N_m is the number of pilot subcarriers. Since $q = \lfloor n/N_m \rfloor$, the channel estimates are obtained only at the frequencies $n = 0, N_m, 2N_m, \ldots, (N_c - 1)$ as shown in Figure 6. Hence, the frequency-domain interpolation described in Section 3.1 is used to obtain the channel gains for all frequencies (i.e., $n = 0 \sim N_c - 1$). N_m-point IFFT is performed on $\{\overline{H}_g(q);\ q = 0 \sim N_m - 1\}$ to obtain the instantaneous channel impulse response $\{\overline{h}(\tau);\ \tau = 0 \sim N_m - 1\}$ as in (9) and then, N_c-point FFT is applied to obtain the interpolated channel gain estimates $\{H_{e,g}(n);\ n = 0 \sim N_c - 1\}$.

3.4. Pilot Sequence Selection. A selection of pilot sequence is an important design issue. If the amplitude of $P(n)$ drops at some frequencies, the noise component in the channel estimate will be enhanced and thereby the estimation accuracy will degrade leading to poor performance. To avoid the noise enhancement, it is desirable that $P(n)$ has constant amplitude irrespective of n. On the contrary, if $P(n)$ is constant for all n, a large amplitude variation may appear in $p(t)$ and consequently, the pilot signal may be distorted due to nonlinear power amplification. In this paper we use Chu sequence [14] as the pilot since the PAPR problem is not present as shown in Figure 7.

3.5. Noise Power Estimation. The noise component at the qth pilot subcarrier can be estimated by subtracting the received pilot component $H_{e,g}(q)P(q)$ from $\overline{R}_g(q)$ as

$$N_{e,g}(q) = \overline{R}_g(q) - H_{e,g}(q)P(q) \tag{11}$$

for $q = 0 \sim N_m - 1$. The noise variance estimate can be obtained as

$$2\sigma_{e,g}^2 = \frac{1}{N_m} \sum_{q=0}^{N_m-1} \left| N_{e,g}(q) \right|^2. \tag{12}$$

Note that in the case of channel estimation scheme presented in Section 3.2, all subcarriers are used as pilots (i.e., $N_m = N_c$).

In what follows, we present MSE analysis of the channel estimator with use of both time-domain first-order filtering and frequency-domain interpolation.

4. Performance Analysis

We have presented pilot-assisted channel estimation schemes in Section 3. The performance of channel estimators presented in Sections 3.2 and 3.3 has already been theoretically investigated in literature; hence, we analyze only the performance of the estimator presented in Section 3.1.

The gth frame's filtered channel gain estimate at the qth subcarrier can be expressed as

$$\overline{H}_g(q) = \gamma H_g(q) + (1 - \gamma)\overline{H}_{g-1}(q) \tag{13}$$

with the initial condition $\overline{H}_0(q) = H_0(q)$ and $0 < \gamma \leq 1$. We define the MSE at nth subcarrier component of the gth frame as $\mathrm{MSE}_g(n) = E[|e_g(n)|^2] = E[|H_{e,g}(n) - H_g(n)|^2]$.

Substituting (9) and (10) into (13), the channel gain estimate is given as

$$\begin{aligned} H_{e,g}(n) = {} & \gamma H_g(n) + (1 - \gamma)\overline{H}_{g-1}(n) \\ & + (1 - \gamma) \sum_{q=0}^{N_m-1} \widetilde{N}_{g-1}(q)\Psi(n, q), \end{aligned} \tag{14}$$

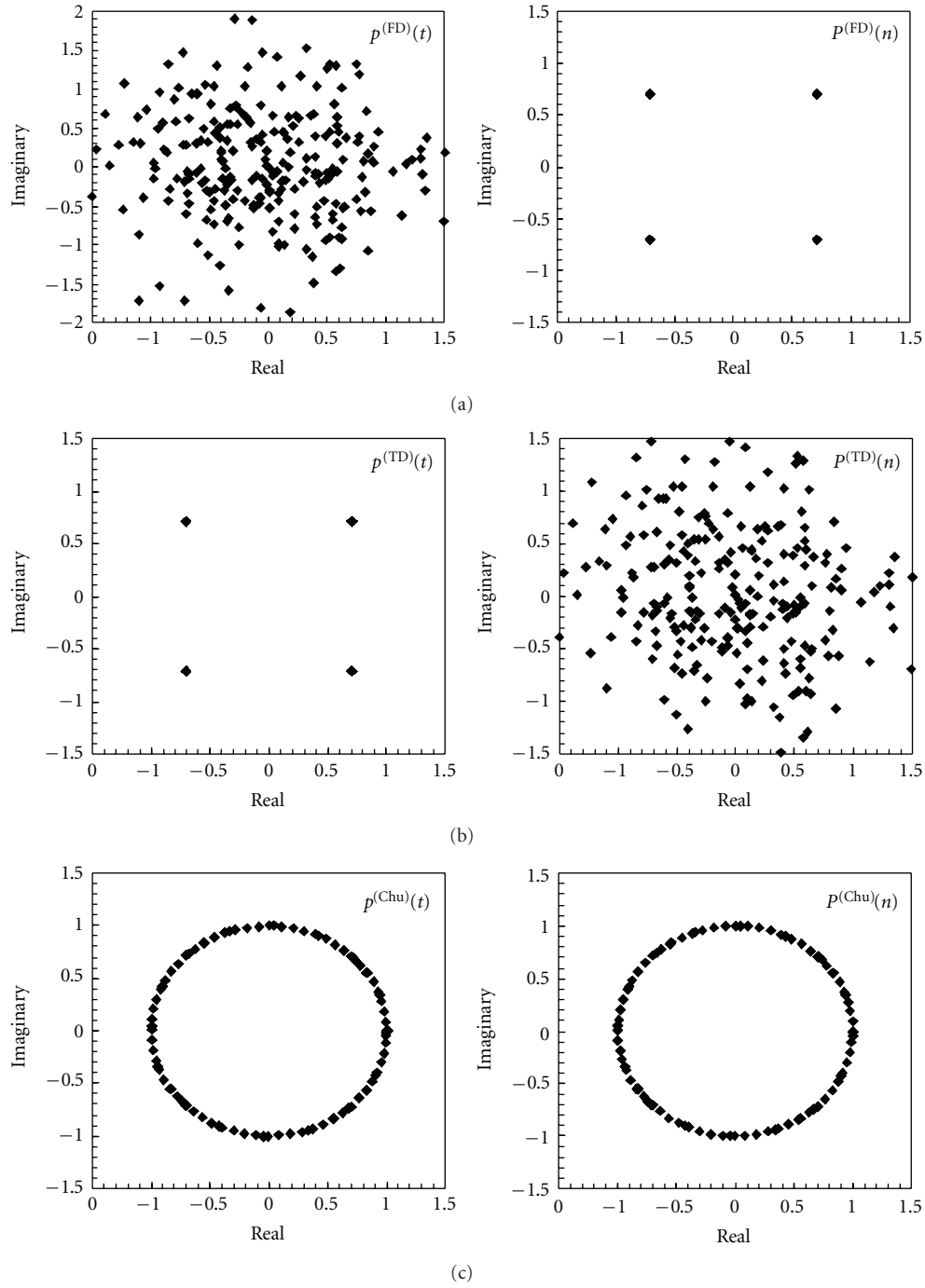

FIGURE 7: Pilot amplitude: (a) constant amplitude in frequency-domain (FD), (b) constant amplitude in time-domain (TD), and (c) constant amplitude in both time- and frequency domains (Chu).

where

$$\Psi(n,q) = \frac{1}{N_m}\frac{\sin(\pi N_m((Kq-n)/N_c))}{\sin(\pi((Kq-n)/N_c))} \times \exp\left[-j\pi(N_m-1)\frac{Kq-n}{N_c}\right] \quad (15)$$

is the frequency-domain interpolation function with $q = \lfloor n/K \rfloor$ for $n = 0 \sim N_c - 1$. Using (14), the $\mathrm{MSE}_g(n)$ of the gth frame's filtered and interpolated channel gain estimate at the nth subcarrier is obtained as

$$\mathrm{MSE}_g(n) = (1-\gamma)^2\mathrm{MSE}_{g-1}(n) + \gamma^2\left(\frac{2E_s}{N_0}\right)^{-1} + 2(\gamma-1)^2\left[R_H(0) - J_0\left(2\pi f_D T_f N_m\right)\right], \quad (16)$$

where $R_H(m-n) = E[H_g(n)H_g^*(m)]$ is the channel frequency-correlation function, $J_0(x)$ is the zeroth order

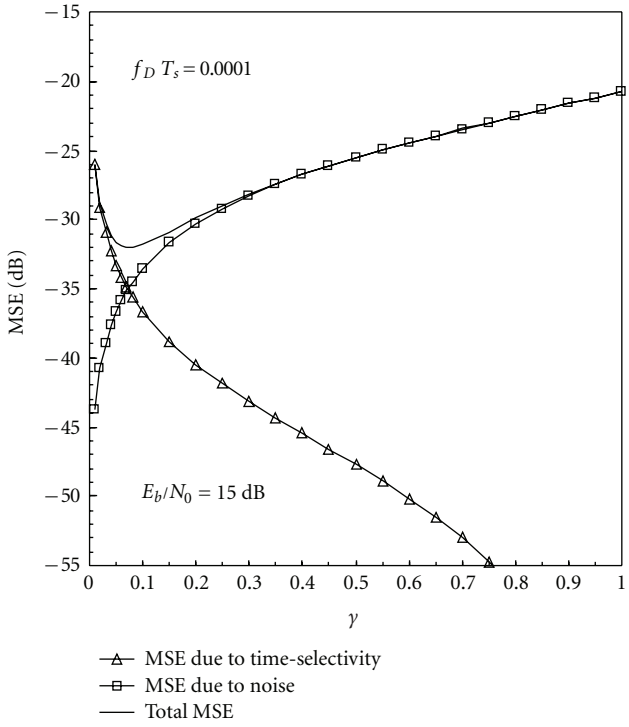

Figure 8: Tradeoff between the noise reduction and robustness against the channel time-selectivity.

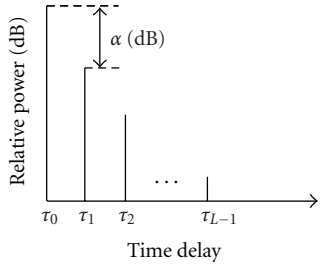

Figure 9: Channel decay profile.

Bessel function of the first kind, and $f_D T_f$ is the normalized Doppler frequency with $1/T_f = 1/T_c N_m$. We assume Jake's isotropic scattering model [15]. It can be seen from (16) that the gth frame's $\mathrm{MSE}_g(n)$ of the channel estimator is a function of the previous $(g-1)$th frame's MSE. To obtain average MSE in a steady-state condition, we let $g \to \infty$ and thus, we obtain

$$\mathrm{MSE} = \frac{\gamma}{(2-\gamma)}\left(\frac{2E_s}{N_0}\right)^{-1} + \frac{2(\gamma-1)^2}{\gamma(2-\gamma)}\left[R_H(0) - J_0\left(2\pi f_D T_f N_m\right)\right]. \tag{17}$$

As shown by (17), the MSE of channel estimator with time-domain first-order filtering and frequency-domain interpolation is not a function of the channel frequency-selectivity and it is only a function of E_s/N_0 and the channel time-selectivity. The first term of (17) represents the influence of AWGN, while the second term represents the influence of the channel time-selectivity. Thus, a tradeoff is present; as the filter coefficient γ increases (decreases), the channel estimator becomes more (less) robust against the channel time-selectivity while on the other hand, the estimator ability to reduce the noise decreases (improves). This tradeoff property computed using (17) is illustrated in Figure 8.

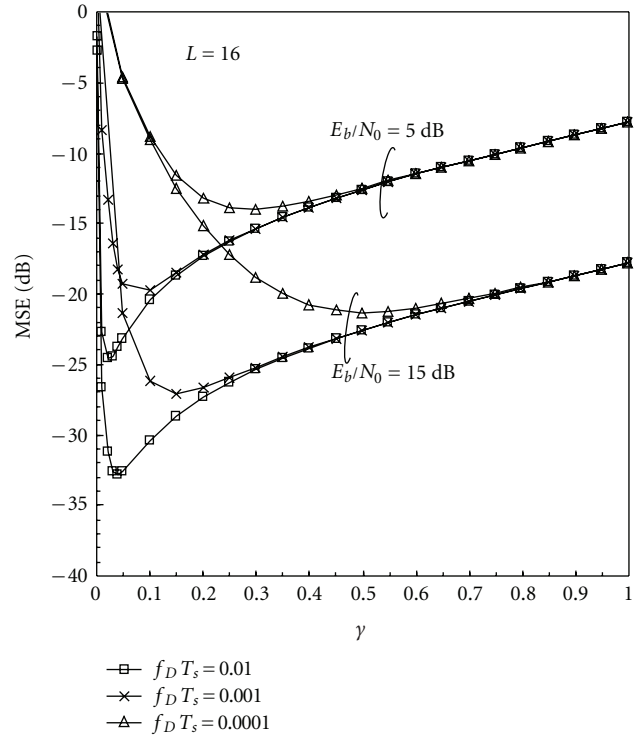

Figure 10: Average MSE performance.

5. Simulation Results and Discussions

Simulation parameters are shown in Table 1. We assume QPSK data-modulation with $N_c = 256$ and $N_m = 16$. Chu sequence is used as the pilot given by $p(t) = \exp(j\pi t^2/N_m)$ for $t = 0 \sim N_m - 1$ [14]. Propagation channel is an $L = 16$-path block Rayleigh fading channel having exponential power delay profile with decay factor α as shown in Figure 9. The zero-mean independent complex path gains $\{h_l;\ l = 0 \sim L-1\}$ remain constant over one OFDM/TDM frame length and vary frame-by-frame. Without loss of generality, we assume $\tau_0 = 0 < \tau_1 < \cdots < \tau_{L-1}$ and that the lth path time delay is $\tau_l = l\Delta$, where $\Delta(\geq 1)$ denotes the time delay separation between adjacent paths. The maximum time delay of the channel is equal to the GI length (i.e., $L = N_g$).

5.1. Optimum γ. Figure 10 shows the average MSE as a function of the time-domain filter coefficient γ with $f_D T_s$ as a parameter for $\alpha = 0$ dB and the average signal energy per bit-to-AWGN power spectrum density ratio $E_b/N_0 = 5$ and 15 dB (i.e., $E_b/N_0 = 0.5 \times (E_s/N_0) \times (1 + N_g/N_c)$). f_D is the maximum Doppler frequency and T_s (= $(N_c +$

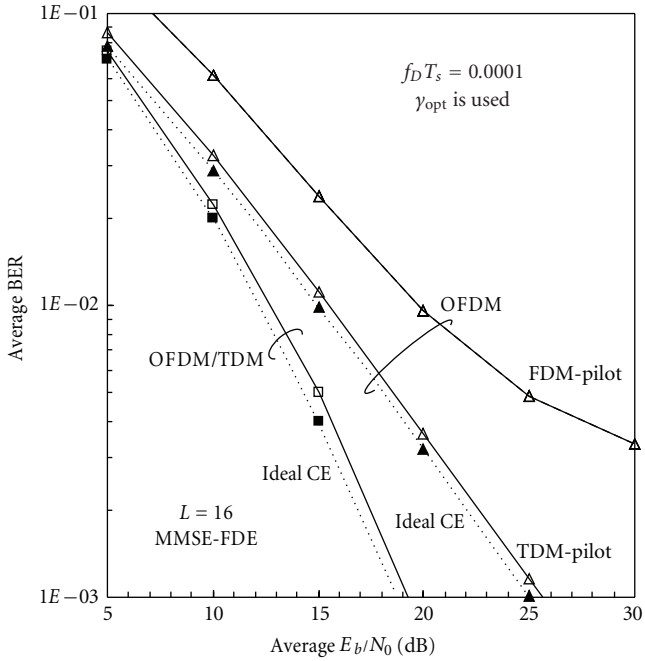

Figure 11: Average BER performance.

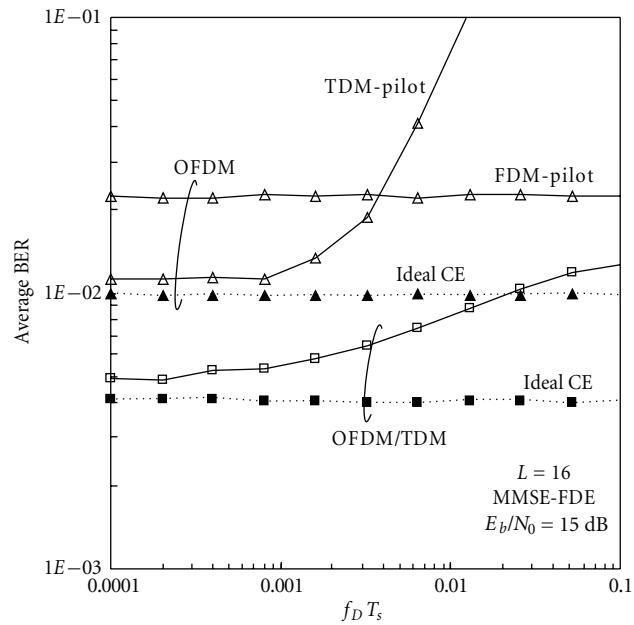

Figure 12: Impact of f_D.

Table 1: Simulation parameters.

Transmitter	Data modulation	QPSK
	Frame length	$N_c = 256$
	IFFT size	$N_m = 16$
	No. of slots	$K = 16$
	GI	$N_g = 16$
Channel	$L = 16$-path fast Rayleigh fading with $\Delta = 1$	
Receiver	FFT size	$N_c = 256$
	FDE	MMSE

$N_g)T_c$) is OFDM/TDM frame length. The figure shows that the proposed channel estimation provides a good MSE performance. As the value of γ decreases, the noise is reduced, but the tracking ability against fading tends to be lost. As $f_D T_s$ increases, the channel varies faster and consequently, the higher γ is required to better track the fading variations. Thus, the optimum value of γ is not only a function of E_b/N_0 but also the channel time-selectivity. As shown in Figure 10, the optimum γ_{opt}, for minimizing the MSE for $E_b/N_0 = 5$ (15) dB is about $\gamma_{\text{opt}} = 0.03$ (0.04), 0.1 (0.15), and 0.3 (0.5) for $f_D T_s = 0.0001$, 0.001, and 0.01, respectively.

5.2. BER Performance. Figure 11 illustrates the average BER performance using the proposed channel estimation as a function of E_b/N_0 for $f_D T_s = 0.0001$ and $\alpha = 0$ dB. The optimum γ is used for each E_b/N_0 value. It can be seen from Figure 10 that the OFDM/TDM with the proposed channel estimation achieves a much better BER performance than OFDM; the required E_b/N_0 for BER $= 10^{-3}$ reduces by about 6.5 dB in comparison with OFDM using TDM-pilot when $f_D T_s = 0.0001$. The E_b/N_0 degradation of OFDM/TDM in comparison to ideal channel estimation is only about 0.6 dB.

The normalized Doppler frequency $f_D T_s$ is an important parameter that affects the BER performance with pilot-assisted channel estimation. To show the advantage of OFDM/TDM over the conventional OFDM, Figure 12 shows the BER performance with proposed channel estimation as a function of $f_D T_s$ for $E_b/N_0 = 15$ dB and $\alpha = 0$ dB. The optimum γ_{opt} is used for each $f_D T_s$ value. For comparison, we also plot curves for OFDM with channel estimation using both FDM-pilot and TDM-pilot. The achievable BER of OFDM/TDM is lower than OFDM, but it slightly increases as $f_D T_s$ increases.

The above performance improvement is obtained at the cost of a slight increase in computational complexity in comparison with conventional OFDM [13].

5.3. Impact of Channel Frequency-Selectivity. The channel frequency-selectivity is a function of channel decay factor α; as α increases the channel becomes less frequency-selective and when $\alpha \to \infty$ it approaches a frequency-nonselective channel (single-path channel). Figure 13 illustrates the average BER performance using the proposed channel estimation as a function of the channel decay factor α.

First we examine the impact of α on the channel estimation accuracy by evaluating the MSE. Figure 13(a) illustrates the dependency of MSE of channel estimation on α when $E_b/N_0 = 15$ dB. The MSE is almost insensitive to $f_D T_s$. Figure 13(b) illustrates the BER dependency on α when $E_b/N_0 = 15$ dB. The BER curve of ideal channel estimation case is also plotted as a reference. It can be seen that, as α increases, the BER slightly increases due to the reduced frequency diversity gain resulting from a weaker channel frequency-selectivity.

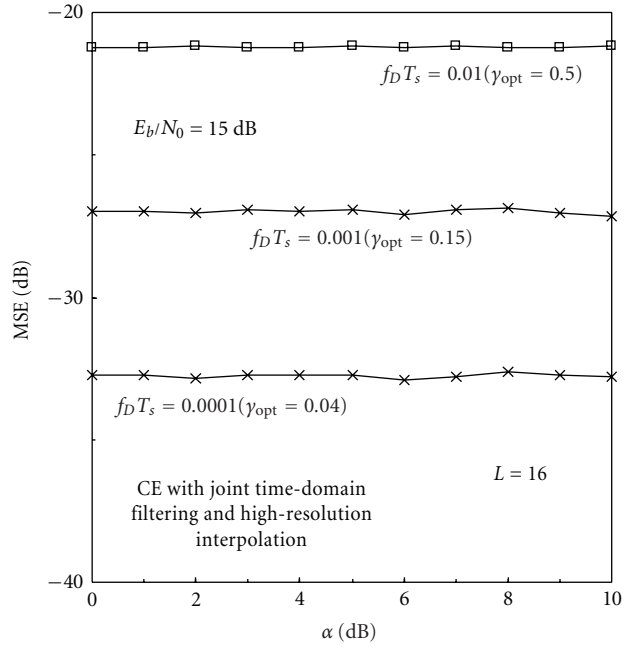

(a) MSE versus α

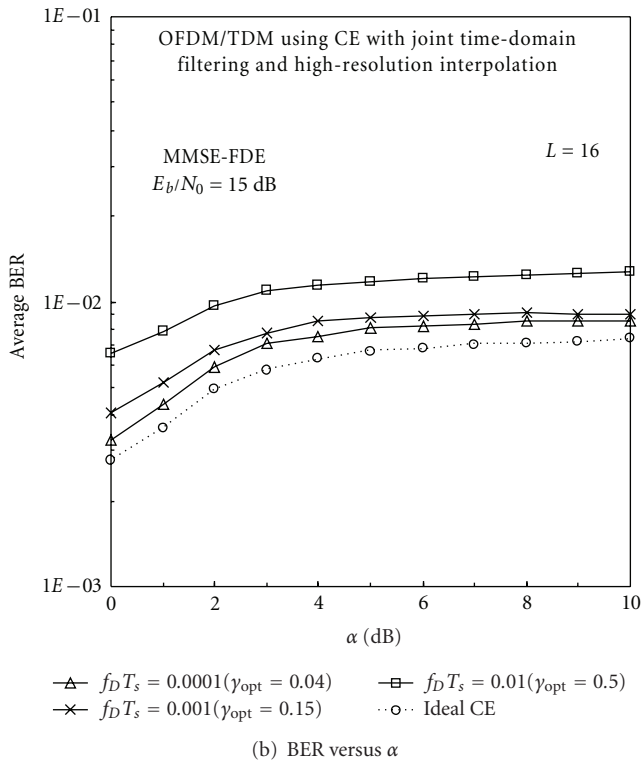

(b) BER versus α

Figure 13: Impact of channel frequency-selectivity.

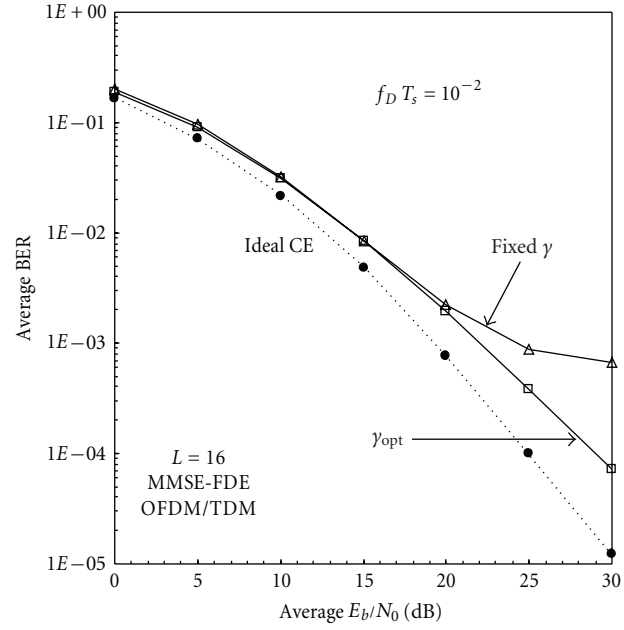

(a) BER versus E_b/N_0

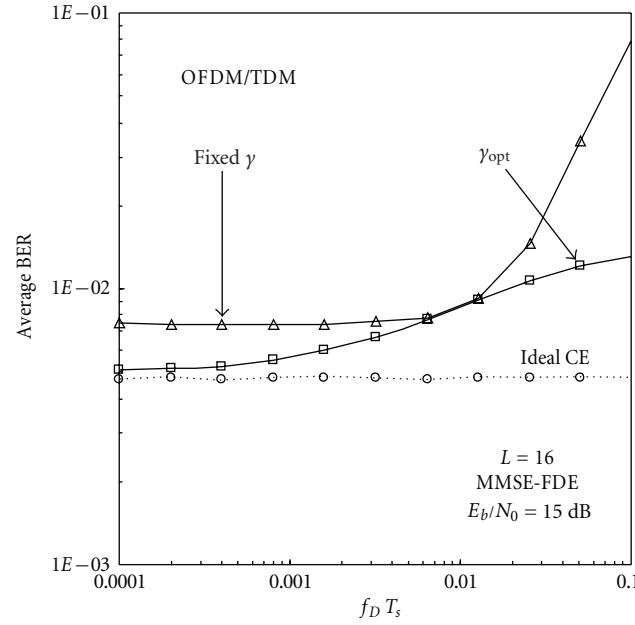

(b) BER versus $f_D T_s$

Figure 14: Fixed γ ($\gamma = 0.5$ at $E_b/N_0 = 15$ dB and $f_D T_s = 10^{-2}$).

5.4. Fixed γ. Since γ is one of the key parameters in the estimator, in this section, we discuss the robustness of the algorithm when γ is fixed. Figure 14 illustrates the average bit error rate (BER) performance with: (i) ideal CE, (ii) optimum γ (i.e., γ_{opt}) and (iii) fixed γ. The performance with ideal CE is illustrated as a reference.

Figure 14(a) illustrates the BER performance as a function of E_b/N_0 at $f_D T_s = 10^{-2}$. The figure shows that for a lower E_b/N_0 (i.e., $E_b/N_0 < 15$ dB), the BER with fixed $\gamma = 0.5$ is almost the same as with γ_{opt}. As expected, γ_{opt} and fixed $\gamma = 0.5$ give the same BER at $E_b/N_0 = 15$ dB because $\gamma = 0.5$ is optimum value at $E_b/N_0 = 15$ dB and $f_D T_s = 10^{-2}$. However, as E_b/N_0 increases (i.e., $E_b/N_0 > 15$ dB), the BER with fixed $\gamma = 0.5$ approaches a floor value of about BER $= 10^{-3}$, while the performance with γ_{opt} consistently improves.

Figure 14(b) illustrates the BER performance as a function of $f_D T_s$ at $E_b/N_0 = 15$ dB. The figure shows that in a slow fading environment (i.e., $f_D T_s < 10^{-2}$) the BER with fixed $\gamma = 0.5$ slightly increases in comparison with γ_{opt}; for $f_D T_s = 10^{-3}$ the BER performance degradation with fixed $\gamma = 0.5$ is as small as 2×10^{-3} in comparison with γ_{opt}. As expected, γ_{opt} and fixed $\gamma = 0.5$ give the same BER at $f_D T_s = 10^{-2}$ because $\gamma = 0.5$ is optimum value at $E_b/N_0 = 15$ dB and $f_D T_s = 10^{-2}$. However, as the value of $f_D T_s$ further increases (i.e., the channel becomes more time selective) the BER rapidly increases as well.

The above results indicate that if a fixed γ is to be used, γ_{opt} at the nominal value of E_b/N_0 and $f_D T_s$ in a considered scenario should be selected as the fixed γ.

6. Conclusions

In this paper, the performance evaluation of OFDM/TDM using MMSE-FDE with practical channel estimation in a fast fading channel was presented. A tracking against fast fading is improved by robust pilot-assisted channel estimation that uses time-domain first-order filtering on a slot-by-slot basis and frequency-domain interpolation. The MSE of the channel estimator using time-domain first-order filtering and frequency-domain interpolation was derived and then, a tradeoff between improving the tracking ability against fading and the noise reduction was discussed. It was shown that the OFDM/TDM using MMSE-FDE provides a lower BER and a very good tracking ability against fading in comparison with conventional OFDM while keeping the same data-rate transmission.

Acknowledgment

This work was supported by Grant-in-Aid for Scientific Research from Japan Society for the Promotion of Science (JSPS).

References

[1] S. Hara and R. Prasad, *Multicarrier Techniques for 4G Mobile Communications*, Artech House, Boston, Mass, USA, June 2003.

[2] C. V. Sinn, J. Gotze, and M. Haardt, "Common architectures for TD-CDMA and OFDM based mobile radio systems without the necessity of a cyclic prefix," in *MS-SS Workshop*, pp. 1–13, DLR, Oberpfaffenhofen, Germany, September 2001.

[3] H. Gacanin, S. Takaoka, and F. Adachi, "Bit error rate analysis of OFDM/TDM with frequency-domain equalization," *IEICE Transactions on Communications*, vol. E89-B, no. 2, pp. 509–517, 2006.

[4] S. Coleri, M. Ergen, A. Puri, and A. Bahai, "Channel estimation techniques based on pilot arrangement in OFDM systems," *IEEE Transactions on Broadcasting*, vol. 48, no. 3, pp. 223–229, 2002.

[5] M.-H. Hsieh and C.-H. Wei, "Channel estimation for OFDM systems based on comb-type pilot arrangement in frequency selective fading channels," *IEEE Transactions on Consumer Electronics*, vol. 44, no. 1, pp. 217–225, 1998.

[6] W. Zhang, X.-G. Xia, and P. C. Ching, "Optimal training and pilot pattern design for OFDM systems in Rayleigh fading," *IEEE Transactions on Broadcasting*, vol. 52, no. 4, pp. 505–514, 2006.

[7] Y.-S. Choi, P. J. Voltz, and F. A. Cassara, "On channel estimation and detection for multicarrier signals in fast and selective Rayleigh fading channels," *IEEE Transactions on Communications*, vol. 49, no. 8, pp. 1375–1387, 2001.

[8] D. Falconer, S. L. Ariyavisitakul, A. Benyamin-Seeyar, and B. Eidson, "Frequency domain equalization for single-carrier broadband wireless systems," *IEEE Communications Magazine*, vol. 40, no. 4, pp. 58–66, 2002.

[9] J. Coon, M. Sandell, M. Beach, and J. McGeehan, "Channel and noise variance estimation and tracking algorithms for unique-word based single-carrier systems," *IEEE Transactions on Wireless Communications*, vol. 5, no. 6, pp. 1488–1496, 2006.

[10] L. Deneire, B. Gyselinckx, and M. Engels, "Training sequence versus cyclic prefix—a new look on single carrier communication," *IEEE Communications Letters*, vol. 5, no. 7, pp. 292–294, 2001.

[11] O. Edfors, M. Sandell, J.-J. Van de Beek, S. K. Wilson, and P. O. Borjesson, "OFDM channel estimation by singular value decomposition," *IEEE Transactions on Communications*, vol. 46, no. 7, pp. 931–939, 1998.

[12] S. Haykin, *Adaptive Filter Theory*, Prentice Hall, Upper Saddle River, NJ, USA, 1996.

[13] H. Gacanin, S. Takaoka, and F. Adachi, "Pilot-assisted channel estimation for OFDM/TDM with frequency-domain equalization," in *Proceedings of the 62nd IEEE Vehicular Technology Conference (VTC '05)*, pp. 554–558, Dallas, Tex, USA, September 2005.

[14] D. C. Chu, "Polyphase codes with good periodic correlation properties," *IEEE Transactions on Information Theory*, vol. 18, no. 4, pp. 531–532, 1972.

[15] W. C. Jakes, *Microwave Mobile Communications*, John Wiley & Sons, New York, NY, USA, 1975.